IEEE ALGERIA SECTION

M'SILA UNIVERSITY IEEE STUDENT BRANCH

IEEE Photonics Society ALGERIA CHAPTER

FACULTY OF TECHNOLOGY

LGE laboratoire de génie électrique

1985 جامعة محمد بوضياف - المسيلة Université Mohamed Boudiaf - M'sila

Certificate of Participation

This is to certify that:

Abdelmalik Zorig

Participated in the ***"The 2nd International Conference of Advanced Technology in Electronic and Electrical Engineering (ICATEEE2025)" held from December 10-11, 2025, at University of M'Sila, Algeria***" with a presentation entitled:

Control of Grid connected PV System Based Paralleled T-type Multilevel Inverters

Co-authors: Said Barkat, Mohammed Belkheiri, Abdelhamid Rabhi, Ismail Ghadbane, Abdelhafid Benyounes.

ICATEEE 2025

December 10-11, 2025, at University of M'Sila, Algeria
https://media.univ-msila.dz/ICATEEE25/

Mohamed Boudiaf University - M'sila
The 2nd International Conference of Advanced Technology in Electronic and Electrical Engineering
ICATEEE2025
10th to 11th December 2025
M'sila
Faculty of Technology

Prof: Ismail GHADBANE

General Chair

Control of Grid connected PV System Based Paralleled T-type Multilevel Inverters

Zorig Abdelmalik
Laboratoire de Génie Électrique
Université Mohamed Boudiaf - M'sila
University Pole, Road Bourdj Bou
Arreiridj, M'sila 28000, Algeria
Abdelmalik.zorig@univ-msila.dz

Barkat Said
Laboratoire de Génie Électrique
Université Mohamed Boudiaf - M'sila
University Pole, Road Bourdj Bou
Arreiridj, M'sila 28000, Algeria
Said.barkat@univ-msila.dz

Belkheiri Mohammed
Laboratoire de Télécommunications, Signaux et Systèmes, Université Amar Telidji, BP 37G, Route de Gardaia
03000, Laghouat, Algérie
m.belkheiri@lagh-univ.dz

Rabhi Abdelhamid
Laboratoire de MIS, Université de Picardie Jules Verne, 33-rue Saint Leu
80039 Amiens Cedex 1-France
abdelhamid.rabhi@u-picardie.fr

Ghadbane Ismail
Laboratoire de Génie Électrique
Université Mohamed Boudiaf - M'sila
University Pole, Road Bourdj Bou
Arreiridj, M'sila 28000, Algeria
ismail.ghadbane@univ-msila.dz

Benyounes Abdelhafid
Laboratoire de Génie Électrique
Université Mohamed Boudiaf - M'sila
University Pole, Road Bourdj Bou
Arreiridj, M'sila 28000, Algeria
abdelhafid.benyounes@univ-msila.dz

***Abstract*— This paper proposes a control method for a photovoltaic generation system based on a three-level boost converter and paralleled three-level T-type inverters (3LT^{2}Is). First, the analytical model of each conversion stage is developed. Then, an appropriate control structure is proposed, which includes active and reactive power control, circulating current suppression, and capacitor voltage balancing. The effectiveness of the proposed control strategy is demonstrated under different operating conditions, including different filter parameters among the parallel inverters, unequal load sharing, and variations in both load and solar irradiation. The obtained results confirm the effectiveness of the proposed control approach on both the DC and AC sides of the system, demonstrating its high capability to suppress circulating currents and ensure capacitor voltage balancing.**

Keywords—Pralled multilevel inverters, three-level boost converter, three-level t-type inverter, circulating current suppression, capacitor voltage balancing.

I. INTRODUCTION

Given the growing global demand for energy, renewable-based renewable energy systems are becoming increasingly attractive, both economically and technologically. However, due to its intermittent nature and distinct output characteristics, power electronic inverters/converters topologies play an essential role in integrating renewable energy sources into distribution grids and in meeting grid connection requirements [1].

Several power inverter topologies have been investigated for the implementation of PV systems based on centralized inverter [1]–[3]. However, these topologies are constrained by limited power ratings, mainly due to the voltage and current capabilities of switching devices.

One approach to overcome the current limitation of switching devices is to connect inverters in parallel.Various works have addressed the parallel operation of two-level inverters/converters and proposed different control strategies to mitigate the circulating current issue associated with with such configurations [4]–[8].

On the other hand, parallel multilevel inverters can overcome both the voltage and current limitations of switching devices. Moreover, compared to two-level inverters, multilevel topologies generate voltage and current waveforms with lower distortion and reduced electromagnetic interference [9]. However, in this topology, the issue of capacitor voltage imbalance is added to the circulating current problem, which further complicates the control strategy.

Recently, various control methods have been proposed in the literature to address both the circulating current and capacitor voltage imbalance issues in the parallel operation of multilevel inverters [10]–[14].

However, the majority of these approaches concentrate mainly on modifying inverter modulation techniques (e.g., PWM, SVPWM) to mitigate the two issues, which makes these strategies ineffective under all operating conditions e.g., varying power factors and modulation indices.

This paper focuses on the overall control of a grid-connected PV system consisting of a DC-DC converter and a parallel multilevel inverter, as shown in Fig. 1 and addresses both circulating current and capacitor voltage imbalance issues.

II. SYSTEM MODELING

A. Modeling of three-level boost converter

Based on Fig.1, the averaged model that describe the dynamic behavior of the input capacitor voltage, the inductor current, and the input neutral-point current is given by:

$$\begin{cases} L_{pv} di_{lpv} / dt = v_{pv} - (1 - D_1) v_{c1} - (1 - D_2) v_{c2} \\ C_{pv} dv_{pv} / dt = i_{pv} - i_{lpv} \\ i_{NP1} = (D_1 - D_2) i_{lpv} \end{cases} \quad (1)$$

where, v_{c1}, v_{c2} are the voltages capacitors; D_1, D_2 are the converter duty cycles.

A. Parallel three-level T-type Inverters

By applying Kirchhoff's law to the circuit of the paralleled 3LT^{2}Is shown in Fig. 1, the model of each 3LT^{2}I module in the *abc* reference frame is obtained as follows:

979-8-3315-6334-9/25/$31.00 ©2025 IEEE

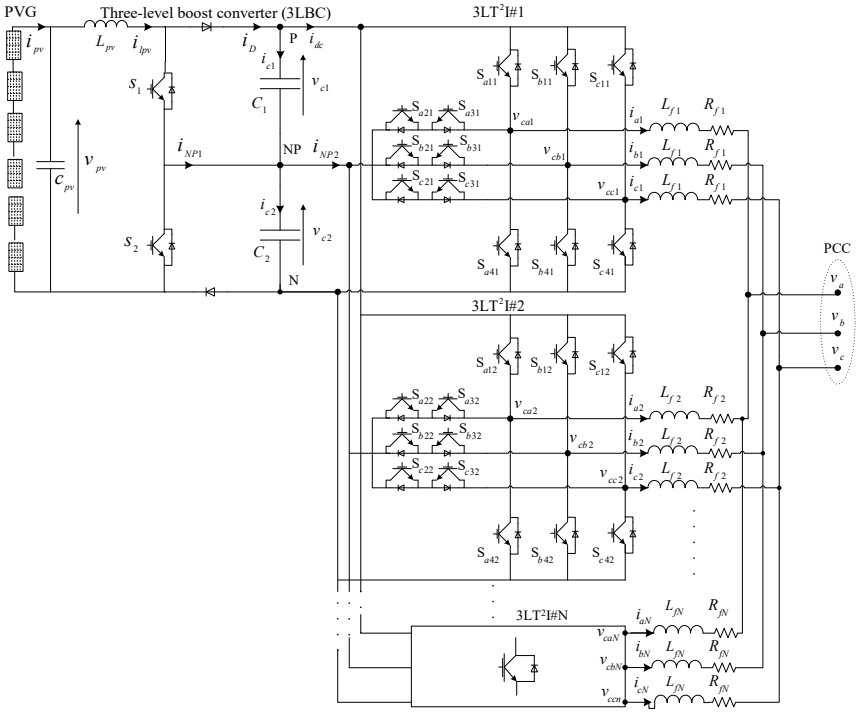

Fig. 1. Diagram of photovoltaic generator (PVG) system made by N parallel three-level t-type inverters sharing the same DC bus with 3LBC.

$$L_{fn}\frac{d}{dt}\begin{bmatrix} i_{an} \\ i_{bn} \\ i_{cn} \end{bmatrix} = -R_{fn}\begin{bmatrix} i_{an} \\ i_{bn} \\ i_{cn} \end{bmatrix} - \begin{bmatrix} v_a \\ v_b \\ v_c \end{bmatrix} + \begin{bmatrix} v_{can} \\ v_{cbn} \\ v_{ccn} \end{bmatrix},\ n = 1,2\ \ldots N \qquad (2)$$

where, v_a, v_b, v_c are voltages at the point of common coupling (PCC); $v_{can}, v_{cbn}, v_{ccn}$ and i_{an}, i_{bn}, i_{cn} are the nth inverter voltages and currents; N is the number of the paralleled inverters; L_{fn}, R_{fn} represent the inductance and its interne resistance, respectively.

The circulating current in each inverter is defined by:

$$i_{0n} = i_{an} + i_{bn} + i_{cn},\ n = 1,2,\ldots, N \qquad (3)$$

By using Park transformation, the average model of the parallel system in the synchronous frame *dq0* can be obtained from (4) as follows:

$$L_{fn}\frac{d}{dt}\begin{bmatrix} i_{dn} \\ i_{qn} \\ i_{0n} \end{bmatrix} = \begin{bmatrix} -R_{fn} & \omega & 0 \\ -\omega & -R_{fn} & 0 \\ 0 & 0 & -R_{fn} \end{bmatrix}\begin{bmatrix} i_{dn} \\ i_{qn} \\ i_{0n} \end{bmatrix} - \begin{bmatrix} v_d \\ v_q \\ v_0 \end{bmatrix} + \begin{bmatrix} v_{cdn} \\ v_{cqn} \\ v_{c0n} \end{bmatrix} \qquad (4)$$

where, $v_d, v_q, v_0, v_{cdn}, v_{cqn}, v_{c0n}$ and i_{dn}, i_{qn} are the components in the *dq0* synchronously rotating frame of the PCC voltage, output voltage and current of inverter n, respectively.

Equation (4) can be rewritten as:

$$L_{f1}\frac{d}{dt}\begin{bmatrix} i_{dn} \\ i_{qn} \end{bmatrix} = \begin{bmatrix} -R_{fn} & \omega \\ -\omega & -R_{fn} \end{bmatrix}\begin{bmatrix} i_{dn} \\ i_{qn} \end{bmatrix} - \begin{bmatrix} v_d \\ v_q \end{bmatrix} + \begin{bmatrix} v_{cdn} \\ v_{cqn} \end{bmatrix} \qquad (5)$$

$$L_{fn}\frac{di_{0n}}{dt} + R_{fn}i_{0n} = v_{c0n} - \sqrt{3}v_0 = d_{0n}v_{dc}/2 - \sqrt{3}v_0 \qquad (6)$$

where, d_{0n} is the zero-sequence duty-cycle of inverter n

III. System Control

A. Circulating current control

To control the circulating current among paralleled three-level inverters, the method proposed in [11] is adopted. This method is based on the dynamic adjustment of the application times of the redundant vectors of the space vector modulation shown in Fig. 2. In this paper, this method is applied to the n 3LT^{2}Is connected to the grid.

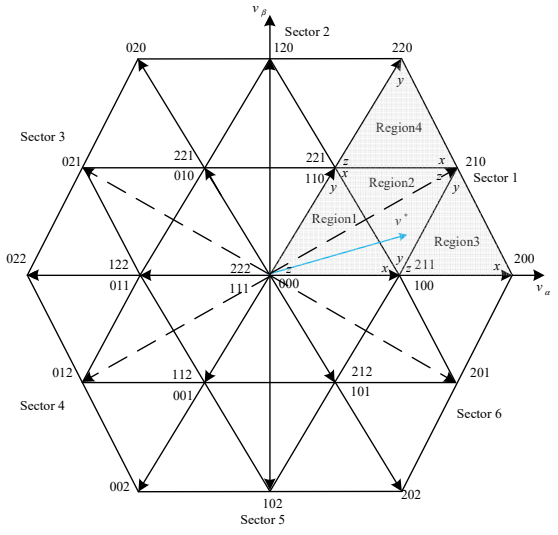

Fig. 2. Switching state vectors of 3LT^{2}I.

Fig. 3 shows the ajustement strategy of the redondnant vectors of region 2 of sector 1. The implementation diagram of the circulating current control including the modified space vector modulation associated with PI controller is illustrated in Fig. 5.

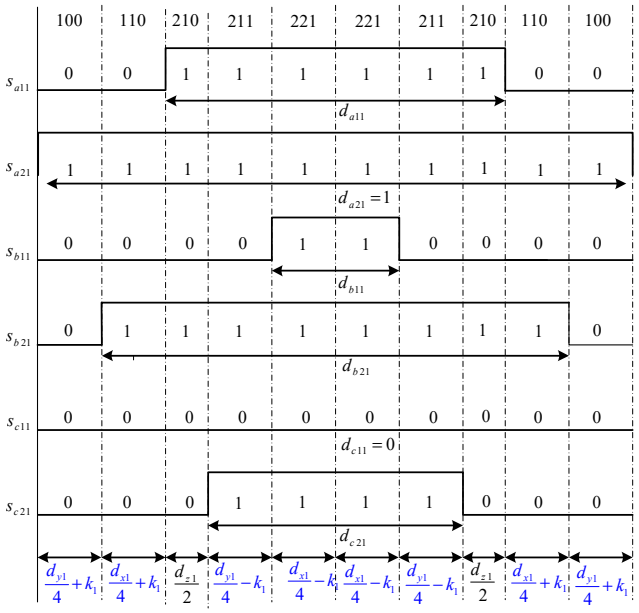

Fig. 3. Adjustment of application time of redundant vectors proposed in [11] (region 2 of sector 1).

B. *Three-level boost control*

The suggested control for the level boost converter, addressing both the DC-link voltage imbalance issue and maximum PV power tracking is shown in Fig. 4.

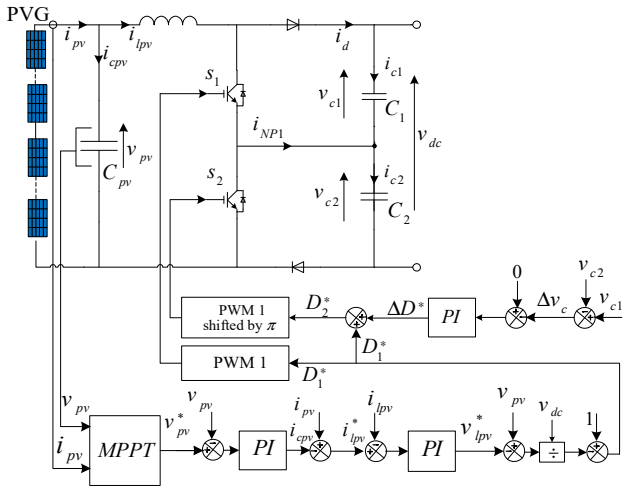

Fig. 4. Proposed three level boost control control addressing both PV power traking and capacitor voltage balancing issues.

Two control loops, based on a PI controller and an MPPT algorithm, are used to determine the duty cycle of the first switch of the converter s_1, as follows:

$$\begin{cases} i_{lpv}^* = i_{pv} - PI(v_{pv}^* - v_{pv}) \\ D_1^* = 1-(v_{pv} - PI(i_{lpv}^* - i_{lpv}))/v_{dc} \end{cases} \tag{7}$$

To control the capacitor voltage imbalance, the voltage difference $\Delta v_c = v_{c1} - v_{c2}$ is fed to a PI controller, which generates an additional duty cycle as follows:

$$\Delta D^* = PI(0-\Delta v_c)/i_{lpv} \tag{8}$$

The additional duty cycle ΔD^* is added to the duty ratio first D_1^* to determine the duty cycle of the second switch $D_2^* = D_1^* + \Delta D^*$. The PWM gating signals are then generated using two carrier signals that are phase-shifted by π from each other.

C. *DC-link voltage control*

The DC-link voltage plays a crucial role in transferring PV power to the grid. As shown in Fig. 5, the error between the squared DC-link voltage and its reference is fed a PI controller to determine the total active power P_{inv}^* to be injected into the grid, as follow:

$$P_{inv}^* = P_{3\text{LBC}} - PI(v_{dc}^{*\,2} - v_{dc}^2) \tag{9}$$

where $P_{3\text{LBC}}$ is the output power of the three-level boost converter.

D. *Control of grid-side of paralled inverter*

The grid-side inverters is controlled by independently controlling the *dq*-axes currents. The d-axis current of the grid-side inverters are used to control the active power flow within the system, while the q-axis current are responsible for controlling the reactive power exchange among the paralleled inverter, the connected loads, and the grid.

The control block diagram of the d-axes and q-axes current loops in the synchronous reference frame is in Fig. 5. The reference currents of each inverter i_d^*, i_q^* can be calculated as function of PCC voltages v_d, v_q , reference of active and reactive powers P_{inv}^*, Q^* as follows:

$$\begin{bmatrix} i_{dn}^* \\ i_{qn}^* \end{bmatrix} = \frac{1}{(v_d^{\,2} + v_q^{\,2})} \begin{bmatrix} v_d & v_q \\ -v_q & v_d \end{bmatrix} \begin{bmatrix} P_{inv}^* \\ Q^* \end{bmatrix} \tag{10}$$

Finally, the control law is given by the following equation:

$$\begin{cases} v_{cdn}^* = v_d + PI(i_{dn}^* - i_{dn}) - L_{fn}\omega i_{qn} = v_d + u'_{dn} - L_{fn}\omega i_{qn} \\ v_{cqn}^* = v_q + PI(i_{qn}^* - i_{qn}) + L_{fn}\omega i_{dn} = v_q + u'_{qn} + L_{fn}\omega i_{dn} \end{cases} \tag{11}$$

From (11), the currents i_{dn}, i_{qn} can be controlled independently by by using PI controllers acting upon u'_{dn} and u'_{qn}, respectively.

IV. Simulation Results

A. *Performance of the overall system under irradiation change*

In this task, the performance of the system in injecting PV power into the grid and compensating the reactive power demand is evaluated under the solar irradiation changes from 1000 W/m^2 to 600 W/m^2.

Fig. 6 shows the waveforms of grid voltage and current, DC link voltage, DC-capacitors voltages, circulating current and active and reactive powers exchanged among grid, load and paralleled inverters.

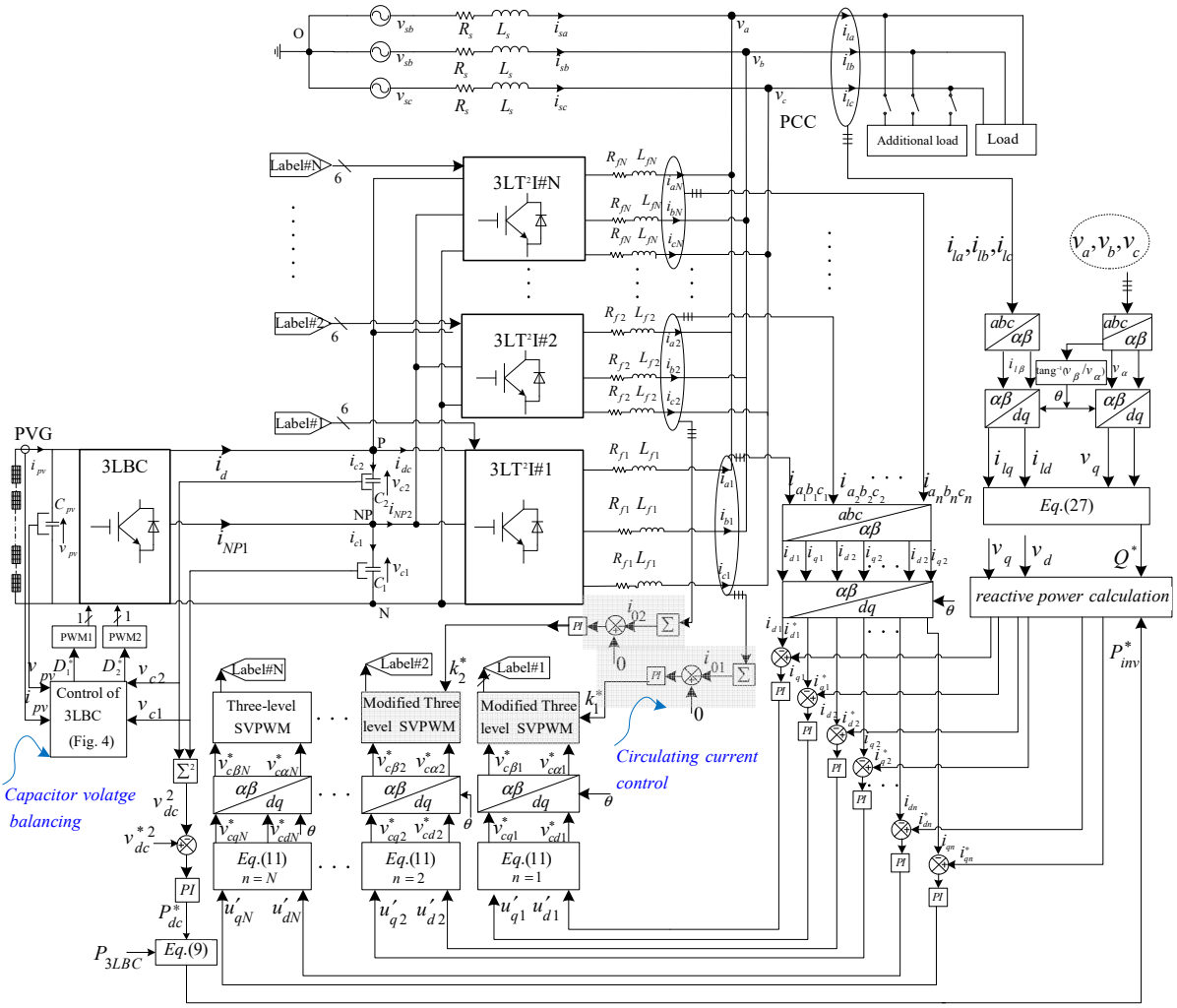

Fig. 5. Control block diagram of the proposed topology with three-level boost converter and N parallel three-level inverters.

Fig. 6(a) shows that, before and after the solar irradiation changes, the paralleled inverter successfully inject the power produced by the PV generator into the grid; since this power is less than the power required to supply the connected load, the remaining active power is therefore absorbed from the grid.

As can be seen in Fig. 6(b), the grid current is in phase with its corresponding voltage, which means that paralleled multilevel inverter successfully compensate the total load reactive power. This can be also noticeable from Fig. 16(c) where there is no reactive power absorbed from the grid.

Fig. 6(d) shows that the DC-link voltage is well regulated even with sudden irradiation changes.

As can be seen in Fig. 6(e), the capacitor voltages are balanced before, during and after irradiation change, which proves the effectiveness of the proposed voltage-balancing control .

Fig. 6(f) shows that even when the paralleled multilevel inverter operate with large differences in the filter parameter values and unequal load sharing, the circulating is almost eliminated.

B. Performance of the overall system under load variation

In this task, the capability of the paralleled inverter in injecting/ compensating the active/reactive power is verified under load variation. The performances of the system are shown in Fig. 7.

As can be seen in Fig. 7(a), at t = 1 s, an additional load is connected, which leads to an increase in the active power absorbed from the grid. This explains the increase in the grid current magnitude shown in Fig. 7(b).

Fig. 7(c) shows that DC-link voltage is well controlled and maintained at its reference value (700 V) even with load variation.

According to Fig. 7(e) the capacitor voltages are balanced before and after load variation which proves the effectiveness of the proposed capacitor voltage-balancing control.

As shown in Fig. 7(f), the circulating currents are successfully eliminated under these challenging conditions, with the parallel inverters operating with differences in filter parameter values, unequal load sharing, and load variations.

V. CONCLUSION

In this paper, a comprehensive control strategy for a photovoltaic system composed by a three-level boost converter and paralleled three-level T-type inverters has been presented. The proposed control strategy includes active power injection, reactive power compensation, circulating current suppression, and capacitor voltage balancing.

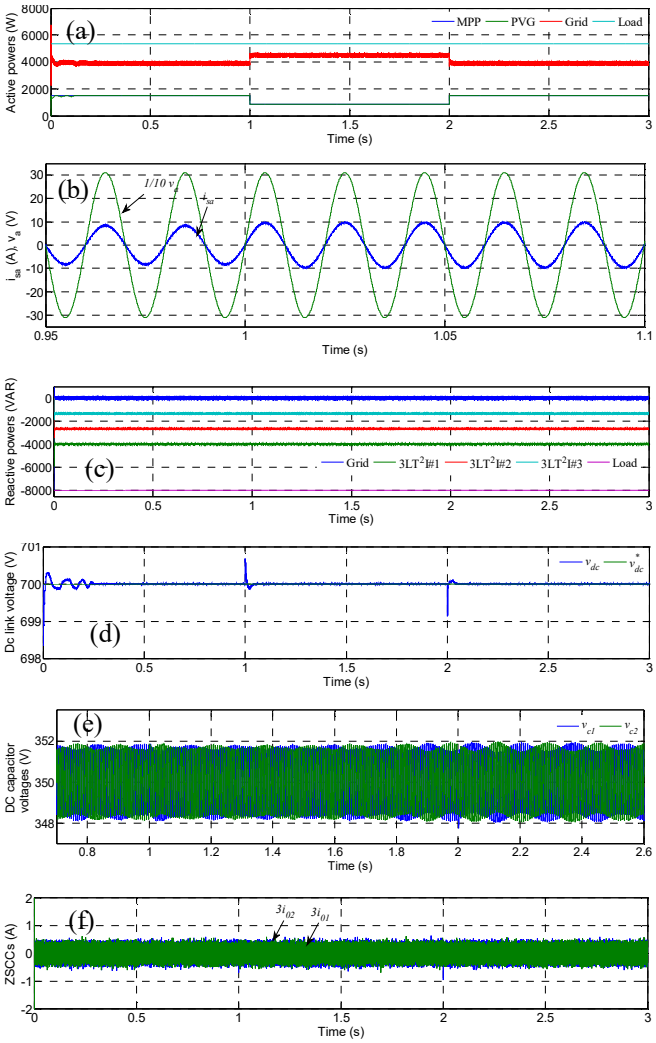

Fig. 6. System Performances under irradiation change: (a) PVG, grid, and load active powers, (b) Grid current and it corresponding voltage (c) Grid, load and 3LT^{2}Is reactive powers , (d) DC-link voltage,(e) DC capacitor voltages, (f) circulating currents.

The obtained results confirm the capability of the proposed strategy to balance the capacitor voltages, eliminate the circulating currents among the paralleled inverters, and ensure a unity power factor. This makes the proposed method a promising solution for reliable and efficient grid-connected PV systems employing parallel multilevel inverters.

Through analytical modeling and detailed simulations, the effectiveness of the proposed control method has been verified under various challenging operating conditions, including mismatched filter parameters, unequal load sharing, and variations in both load and solar irradiation.

REFERENCES

[1] E. Pouresmaeil, C. Miguel-Espinar, M. Massot-Campos, D. Montesinos-Miracle, and O. Gomis Bellmunt, "A control technique for integration of DG units to the electrical networks," IEEE Trans. Ind. Electron., vol. 60, no. 7, pp.2881–2893, Jul. 2013.

[2] N. Hamrouni, M. Jraidi, and A. Chérif, "New control strategy for 2-stage grid-connected photovoltaic power System," Renewable Energy, vol. 33, no. 10, pp. 2212–2221, Oct. 2008.

[3] J. M. Kwon, B. H. Kwon, and K. H. Nam, "Three-phase photovoltaic system with three-level boosting MPPT control," IEEE Trans. Power Electron., vol. 23, no. 5, pp. 2319–2327, Sep. 2008.

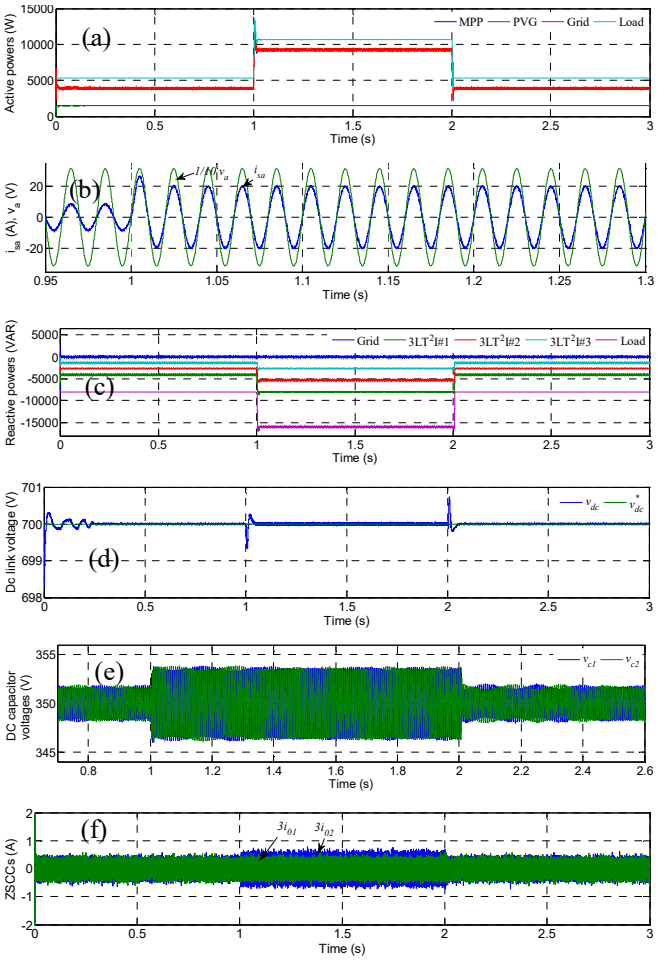

Fig. 7. System Performances under load variation: (a) PVG, grid, and load active powers, (b) Grid current and it corresponding voltage (c) Grid, load and 3LT^{2}Is reactive powers , (d) DC-link voltage,(e) DC capacitor voltages, (f) circulating currents.

[4] F. Wang, Y. Wang, Q. Gao, C. Wang, and Y. Liu, "A Control Strategy for Suppressing Circulating Currents in Parallel-Connected PMSM Drives With Individual DC Links," IEEE Trans. Power Electron., vol. 31, no. 2, pp. 1680-1691, Feb. 2016.

[5] Z. Zhang, A. Chen, X. Xing, and C. Zhang, "A novel model predictive control algorithm to suppress the zero sequence circulating currents for parallel three-phase voltage source inverters," in Proc. IEEE APEC. Conf.Long Beach, Mar. 20–24, 2016, pp. 3465–3470.20-24 March 2016.

[6] G. Gohil, R. Maheshwari, L. Bede, T. Kerekes, R. Teodorescu, M. Liserre, and F. Blaabjerg, "Modified discontinuous PWM for size reduction of the circulating current Filter in parallel interleaved converters," IEEE Trans. on Power Electron., vol. 30, no. 7, pp. 3457-3470, July 2015.

[7] Z. Xueguang, Z. Wenjie, C. Jiaming, and X. Dianguo, "Deadbeat control strategy of circulating currents in parallel connection system of three-phase PWM converter," IEEE Trans. Energy Convers., vol. 29, no. 2, pp. 406–417, Jun. 2014.

[8] X. Wang, F. Zhuo, J. Li, L. Wang, and S. Ni, "Modeling and control of dual-stage high-power multifunctional PV system in d–q–o coordinate," IEEE Trans. Ind. Electron., vol. 60, no. 4, pp. 1556–1570, Apr. 2013.

[9] M. Schweizer and J. W. Kolar, "Design and implementation of a highly efficient three-level T-type converter for low-voltage applications," IEEE Trans. Power Electron., vol. 28, no. 2, pp. 899–907, Feb. 2013.

[10] Y. Xing, Y. Li, W. Qin, J. Chen, and C. Zhang, "An optimized zero-sequence voltage injection method for eliminating circulating current and reducing common mode voltage of parallel-connected three-level converters," IEEE Trans. Ind. Electron., vol. 67, no. 8, pp. 6583-6596, Aug. 2020.

[11] A. Zorig, S. Barkat, A. Rabhi and M. Belkheiri, " Circulating currents control method for paralleled three-level NPC inverters," Electr. Eng., vol. 106, pp.7709–7718, May 2024.

[12] Q. Zhang, X. Xing, and K. Sun, "Space vector modulation method for simultaneous common mode voltage and circulating current reduction in parallel Three-Level inverters," IEEE Trans. Power Electron., vol. 34, no. 14, pp. 3053 - 3066, Apri. 2019.

[13] L. Ping, Z. Xing, W. Fusheng, S. Zhangping, "Control of circulating current and neutral-point potential balancing in two parallel three-level NPC inverters," in Proc. IEEE TENCON. Conf., Xi'an, China, Oct. 22–25, 2013, pp. 1–4.

[14] Z. Shao, X. Zhang, F. Wang, and R. Cao, "Modeling and elimination of zero-sequence circulating currents in parallel three-level T-type grid-connected inverters," IEEE Trans. Power Electron., vol. 30, no. 2, pp. 1050–1063, Feb. 2015.